Preparation of Polyacrylate-Clay Nanocomposites by In-Situ Polymerization and Heterocoagulation

Yijin Xu, William J. Brittain

Department of Polymer Science, University of Akron, Akron, Ohio 44325-3909

Received 25 November 2005; accepted 13 January 2006
DOI 10.1002/app.24187

ABSTRACT: Polyacrylate-clay nanocomposites were prepared by an *in situ* polymerization method followed by heterocoagulation. In the heterocoagulation method, a cationic polyacrylate emulsion was prepared by emulsion polymerization using a cationic initiator in the presence/absence of free surfactant, cetyl trimethylammonium bromide (CTABr), followed by mixing with an aqueous clay slurry. WAXD results and TEM images suggest that morphologies of these nanocomposites depend on preparation method, mixing method, and the amount of free surfactant. TG-DTG analyses demonstrate the improvement in thermal stability of these nanocomposites, while DSC results indicate no significant changes in glass transition temperature of these nanocomposites. © 2006 Wiley Periodicals, Inc. J Appl Polym Sci 101: 3850–3855, 2006

Key words: elastomers; emulsion polymerization; organoclay; nanocomposite

INTRODUCTION

Since the early work on Nylon-clay nanocomposites,[1–3] polymer-layered silicate nanocomposites (PLSNs) have attracted great interest in both industrial and academic labs because of the improvements in mechanical, electrical, barrier, and thermal properties when compared with micro- and macrocomposite counterparts, which result from the molecular level interactions, nanoscale dimensions, and high aspect ratio of the silicate.[4–9]

Recently, some research has shifted to the field of rubber–clay nanocomposites, because of potential mechanical, thermal, and permeability improvements. In the preparation of rubber–clay nanocomposites, four techniques have been reported: solution mixing,[10–14] melt compounding,[15–29] *in situ* polymerization,[30–35] and latex cocoagulation with aqueous clay slurry.[36–41] In terms of economics and environment, the solution route is restricted to laboratory research. For melt-compounding method, the clay should be first modified with organic surfactant through the cationic exchange reaction to increase the miscibility between clay surface and polymers; however, the melt process is often accompanied by surfactant decomposition and most nanocomposites prepared by this method have intercalated or intercalated/exfoliated mixed structures. In the preparation of thermoset–clay and thermoplastics–clay nanocomposites by *in situ* polymerization, the clay surface also needs to be modified so that the prepolymer/monomer can more easily intercalate into the gallery of clay platelets. It is difficult to obtain exfoliated structures by this method. Latex compounding or latex cocoagulation with aqueous clay slurry (heterocoagulation method).[42,43] Literature methods for the preparation of rubber–clay nanocomposites by latex compounding use a negatively charged latex, which is the same charge as the clay surface; thus the interaction is repulsive. Unfavorable electrostatics between the surfaces of latex particle and clay platelets may be the main reason for the intercalated structures of these rubber–clay nanocomposites.

Acrylate rubbers are widely used in engine and transmission seals, gaskets and O-rings because of their good ozone and heat resistance. However, it is difficult to achieve a good balance between oil resistance, low temperature properties, and abrasion resistance. Previous reports demonstrated that the incorporation of clay platelets into rubber–clay nanocomposites improved the barrier properties, thermal stability, solvent resistance, and abrasion properties.[4,15,17,27,28,31,35,39] To the best of our knowledge, there are only three papers reporting the preparation of polyacrylate–clay nanocomposites. Reference 33 uses trimethylol triacrylate as the monomer, and Ref. 34 used butyl acrylate as the monomer; both groups reported an *in situ* polymerization. Reference 35 used an *in situ* emulsion polymerization in the presence of anionic surfactant and initiator with bentonite as a pickering coemulsifier. In all three cases, the final

---

Correspondence to: W. J. Brittain (wjbritt@uakron.edu)
Contract grant sponsor: DURINT on Microstructure, Processing and Mechanical Performance of Polymer Nanocomposites; contract grant number: F49620–01-1–0447.

Journal of Applied Polymer Science, Vol. 101, 3850–3855 (2006)

nanocomposites had an intercalated structure or intercalated/exfoliated mixed structure.

In our research group, we created a method called heterocoagulation where a cationic emulsion latex was first prepared followed by mixing with an aqueous clay slurry; a nanocomposite is obtained by electrostatic interactions.[42,43] Poly(methyl methacrylate) and polystyrene clay nanocomposites with fully exfoliated structures were prepared by this method.[42–44] In comparison with the latex compounding results, we think that the opposite surface charges of the cationic latex and clay platelet facilitates the exfoliation. In a previous paper, we also reported that exfoliated poly(methyl methacrylate) clay nanocomposites could be prepared by *in situ* polymerization with 2,2′-azobis(2-amidinopropane) dihydrochloride as inisurf (acting as both initiator and surfactant) and clay as pickering coemulsifier.[42] In the present article, we report the morphology and thermal properties of polyacrylate–clay nanocomposites prepared by *in situ* polymerization and heterocoagulation.

EXPERIMENTAL

Materials

Montmorillonite, GelWhite GP® with a cationic exchange capacity of 92 mmol/100 g, was provided by Southern Clay Products. 2,2′-Azobis (2-amidinopropane) dihydrochloride (V-50), provided by Wake Pure Chemical Industries, was used without further purification. Cetyltrimethylammonium bromide (CTABr) was obtained from Aldrich and used as received. Ethyl acrylate (EA) and butyl acrylate (BA) from Aldrich were purified by passage through basic alumina oxide to remove the radical inhibitor before use. Deionized water was used in all the experiments.

Instrumentation

Thermogravimetric analysis (TGA) was performed on a Hi-Res TGA 2950 thermograimetic analyzer (TA instruments) ranging from 25 to 800°C at a heating rate of 20°C/min. Differential scanning calorimetry (DSC) experiments were run on a TA Instruments DSC 2920 modulated DSC under a nitrogen atmosphere. A hermetically sealed sample was heated from −65°C (for PEA) or −95°C (for PBA) to 150°C at a ramping rate of 10°C/min; after the first run it was removed and quickly cooled to room temperature. We report the results from second run in this paper. Wide angle X-ray diffraction (WAXD) results were obtained on a Rigaku diffractometer equipped with a rotating-anode generator system using Cu Kα radiation (λ = 1.5418 Å) at the scanning rate of 4°/min ranging from 1.5° to 10°, and the operating current was 150 mA and voltage was 50 kV. Transmission electron microscopy (TEM) experiments were performed on a TECNNAI TEM (FEI) at 120 kV accelerating voltage. The samples were cryo-ultramicrotomed with a diamond knife on a Reichert Ultracuts (Leica) microtome at −65°C (for PEA) or −90°C (for PBA) to give ~50 to 70 nm thick sections.

In situ polymerization with V-50 modified clay

A typical procedure for the *in situ* polymerization of EA and BA is as follows. A four-necked 250 mL round-bottomed flask was equipped with a mechanical stirrer, argon inlet, thermometer and refluxing condenser. A prescribed amount of clay was added to 100 mL of argon-purged distilled water and the slurry was mechanically stirred at 70°C overnight. V-50 (0.38 g) in 20 mL of distilled water was added dropwise; after 30 min, 20 mL of monomer (EA, BA, or EA/BA mixture, 1:1 v/v relative to water) was added to the dispersion. The polymerization was carried out at 70°C for 6 h while stirring at 300 rpm. The polymerization was stopped by cooling to room temperature. After filtration and successively washing with distilled water, the composite was collected and dried in vacuum at room temperature until constant weight.

Preparation of cationic polyacrylate latex

A typical procedure is as follows. A four-necked 500 mL Pyrex reaction kettle was equipped with a mechanical stirrer, argon inlet, thermometer, and refluxing condenser. Deionized water (250 mL), 50 g of purified EA, 0.11 g of CTABr, and 0.82 g of AIBA were added. The reaction contents were purged with argon for 40 min while stirring at 300 rpm followed by heating at 70°C for 6 h. The polymerization was stopped by cooling the reaction to room temperature.

Heterocoagulation

Before the heterocoagulation process, 1% (w/w) clay slurry was prepared by suspending clay in water with rigorous stirring overnight. A predetermined amount of cationic latex and clay slurry were mixed together in a beaker while stirring. The mixture was stirred for 3 h and then allowed to stand until the water had evaporated. The nanocomposite was dried at room temperature *in vacuo* until constant weight.

Sample preparation for TEM

Two methods were used to prepare the sample for microtoming. To preserve the morphology after heterocoagulation, one method involved melting the composite until we obtained a continuous sheet. The other method was to compression mold the composites at 120°C to get a film; however, we believe that

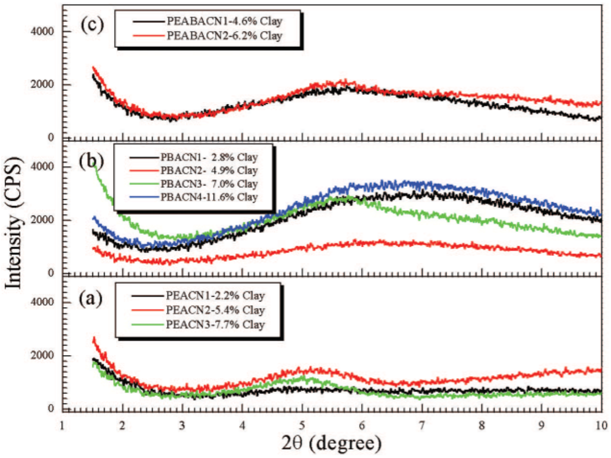

Figure 1 WAXD patterns of polyacrylate–GP nanocomposites. (PEACN, PBACN, and PEABA correspond to PEA–clay, PBA–clay, and poly(EA-*co*-BA)–clay nanocomposites, respectively. "PEACN1–2.2% Clay" means sample 1 of PEA–GP nanocomposites, and 2.2% is the residue determined by TGA at 800°C in air atmosphere. [Color figure can be viewed in the online issue, which is available at www.interscience.wiley.com.]

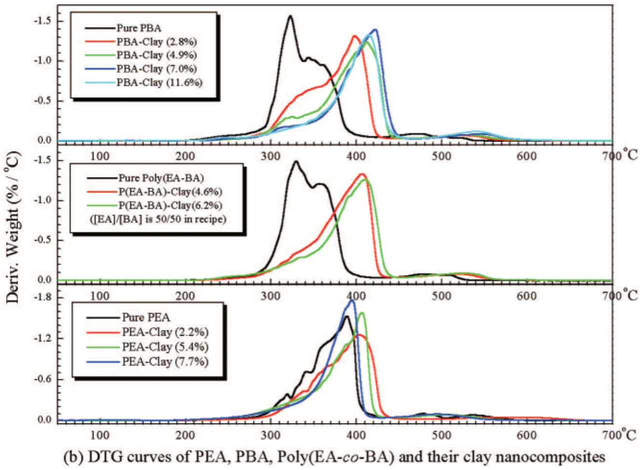

Figure 2 DTG plots of PEA–GP, PBA–GP, and poly(EA-*co*-BA)–GP nanocomposites. The values in parentheses are the residues determined by TGA at 800°C in air atmosphere. [Color figure can be viewed in the online issue, which is available at www.interscience.wiley.com.]

this produces a different arrangement of the clay platelets due to sheer stress.

RESULTS AND DISCUSSION

Polyacrylate-clay nanocomposites via *in-situ* polymerization

Figure 1 shows the WAXD patterns of the polyacrylate–clay nanocomposites prepared by *in situ* polymerization method. From Figure 1(a), it can be seen that for all polyacrylate–GP nanocomposites, there are broad peaks. For PEA–GP nanocomposites [Fig. 1(a)], the gallery spacing is 1.7 nm similar to the PBA–GP nanocomposites [Fig. 1(b)]; the broad peaks centered at $2\theta = 5.5°$ correspond to a gallery spacing of 1.6 nm. For PEABA–GP nanocomposites, the peaks became broader and the gallery spacing is 1.47 nm. Compared with the 1 nm gallery spacing of the pristine clay, these results suggest the formation of intercalated nanocomposites. TEM results indicated that, for PEA–GP and PBA–GP nanocomposites, there is some extent of exfoliation, while for poly(EA-*co*-BA)–GP nanocomposites the intercalated structure dominates.

Figure 2 displays the DTG plots of the polyacrylate–GP nanocomposites. Although there was some improvement in PEA–GP nanocomposites, the improvement is not as significant as the PBA–GP nanocomposites, in which the main decomposition temperature shifted to temperatures 100°C higher than pure PBA. In poly(EA-*co*-BA)-GP nanocomposites, the thermal stability is observed in a decrease of the first decomposition peak, even though the improvement of the end decomposition temperature is smaller than the PBA–GP nanocomposites. These improvements in thermal stability of PEA–GP and PBA–GP nanocomposites were observed previously[33,35]; the different decomposition patterns of pure PEA and PBA of our samples may be due to the different initiator and surfactant used in our *in situ* polymerizations.

Figure 3 summarizes the T_g's (glass transition temperatures) of polyacrylate–GP nanocomposites determined by DSC. For both PEA–GP and poly(EA-*co*-BA)–GP nanocomposites, the change of glass transition temperature in the nanocomposites is negligible; in the PBA–GP nanocomposites, the increase is only

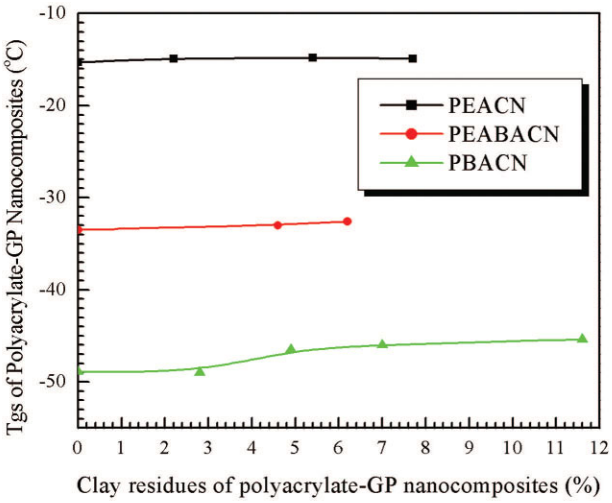

Figure 3 Glass transition temperature comparison of polyacrylate–GP nanocomposites with respect to clay loadings. [Color figure can be viewed in the online issue, which is available at www.interscience.wiley.com.]

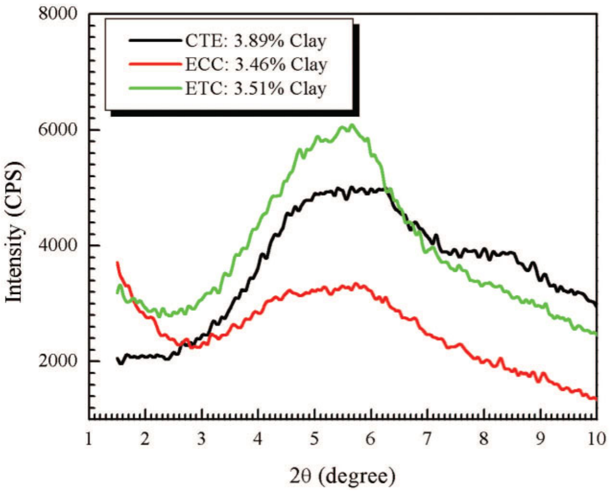

Figure 4 WAXD comparison of poly(EA-*co*-BA)–GP nanocomposites prepared by different mixing methods. (The feed ratio of EA/BA is 40/60, and the cationic latex was prepared by emulsifier-free emulsion polymerization, without the presence of CTABr.) [Color figure can be viewed in the online issue, which is available at www.interscience.wiley.com.]

4°C at a clay loading of 11.6% (from −48.9 to −45.4 °C). This is a positive result because it is desirable to improve the properties of the polyacrylate–clay nanocomposites without sacrificing elasticity.

Synthesis of polyacrylate-clay nanocomposites by heterocoagulation

We have found that fully exfoliated polyacrylate–GP nanocomposites cannot be obtained via *in situ* polymerization, even though exfoliated poly(methyl methacrylate)–GP nanocomposites[42,43] were successfully obtained with this method. The heterocoagulation method has been widely used in the synthesis of inorganic/organic and organic/organic nanocomposites; the method relies on electrostatic interactions between the latex and filler.[43] There are some reports about the use of heterocoagulation method in preparing rubber (natural and synthetic) and clay nanocomposites. However, because of the anionic property of those reported lattices, only intercalated structures were observed.[36–41] When the surface charge was cationic, which is opposite to the anionic charge of the clay surface, exfoliated structures were obtained.[42–44] The reported examples are for thermoplastic-clay nanocomposites (PMMA and polystyrene clay nanocomposites); we have explored the heterocoagulation method to develop fully exfoliated polyacrylate–clay nanocomposites.

Effect of mixing process on the morphology

In the heterocoagulation method, there are three possible mixing processes: addition of emulsion to clay slurry (ETC), addition of clay slurry to emulsion (CTE), and addition of emulsion and clay slurry simultaneously to a beaker with some water (ECC). There are three competitive processes that potentially exist during heterocoagulation[43]: cationic exchange reactions between latex and clay platelets (heterocoagulation), the homocoagulation between clay platelets, and the homocoagulation between cationic latex particles, as well as the low glass transition temperature of acrylate rubbers. Therefore, we studied the effect of mixing on the morphology of acrylate rubber–clay nanocomposites. Figures 4 and 5(a) shows the WAXD comparison of poly(EA-*co*-BA)–GP and PEA–GP nanocomposites by different mixing methods; the results clearly indicate that ECC is the best method to prepare acrylate rubber–clay nanocomposites with exfoliated structure. We speculate that the ECC mixing process is preferred because it is easier to control the instantaneous ratio of clay platelets to latex particles, thus minimizing homocoagulation.

Effect of free surfactant on the morphology

During the heterocoagulation process, the final morphology of the composite was determined by several factors, which include surface charge and ζ-potential of the two colloidal particles, particle size, and particle number ratio (PNR) of the two emulsions. In the cationic latex–clay colloid system, the situation becomes more complicated because of the instability of clay colloid. The presence of most inorganic salts (e.g., NaCl, $CaCl_2$, and $AlCl_3$), alcohols, organic and polymeric cations will cause the coagulation of clay colloids. The addition of electrolyte also causes the coagulation of emulsion particles. It is well-known that the

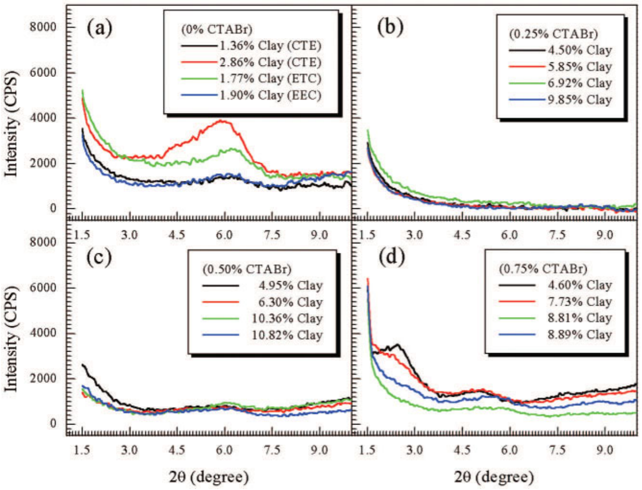

Figure 5 WAXD patterns for the PEA–GP nanocomposites from the emulsions with different amounts of free surfactant CTABr. [Color figure can be viewed in the online issue, which is available at www.interscience.wiley.com.]

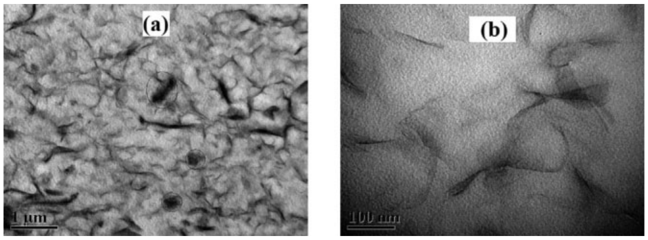

Figure 6 Low and high magnification TEM images of PEA–GP (4.95% clay) nanocomposite (0.50% free surfactant with respect to monomer, and no pressing during sample preparation for TEM).

amount of free surfactant used in emulsion polymerization will affect the latex particle numbers, the particle size, and surface charge density. Also, the free surfactant is not totally adsorbed on the latex particle surface, some of the surfactant dissolves in aqueous phase and there is a dynamic equilibrium between adsorption and desorption from the latex particle surface. Therefore, we studied the effect of free surfactant on the morphology of polyacrylate–GP nanocomposites.

Four batches of emulsions were prepared. The amounts of distilled water, monomer, and V-50 were kept the same in all the four recipes while 0, 0.25, 0.5, and 0.75% of free surfactant CTABr with respect to BA was used in different batches. Figure 5 summarizes the WAXD results for the polyacrylate–GP nanocomposites from those four emulsions. Figure 5(a) indicates that each PEA–GP nanocomposite from emulsifier-free emulsion polymerization displayed a peak at $2\theta = 6°$ corresponding to a gallery spacing of 1.47 nm consistent with an intercalated structure. Fully exfoliated structures were suggested based on WAXD results in Figure 5(b) for the PEA–GP nanocomposites from the emulsion with 0.25% of free surfactant. Figure 5(c) suggests the formation of some intercalated structures in the nanocomposites when the free surfactant amount increased to 0.50% with respect to monomer in the emulsion polymerization. An interesting phenomenon was observed when the free surfactant amount was further increased to 0.75%. In these nanocomposites, intercalated structures were found at lower clay loadings while exfoliated structures were observed at higher clay loadings; this is opposite of the usual trend for changes in clay loadings. The increase of free surfactant amount increases the surface charge density, which leads to stronger interaction between latex particles and clay platelets; however, a further increase of free surfactant may also lead to higher concentration of free surfactant in aqueous phase, which may promote coagulation and precipitation of the clay platelets.

To further investigate the morphology of the PEA–GP nanocomposites prepared by heterocoagulation method, TEM experiments were performed. Figures 6(a)–6(c) show the low and high magnification TEM pictures of PEA–GP nanocomposite with 4.95% clay; the sample was heated to melt state without pressing (see experimental section). From Figure 6(a), we can see that the clay platelets are randomly dispersed in the rubber matrix; the black spots in circles are the salt particles from cation exchange reaction (not shown here). We also see few tactoids in this picture. Figure 6(b) clearly shows the deformation of single clay platelets in rubber matrix, while Figure 6(c) indicates that the spacing between clay platelets is more than 10 nm, although the image is not well focused because of the deformation of rubber matrix. Figures 7(a) and 7(b) are the TEM images for PEA–GP nanocomposites with 5.85 and 9.85% clay loadings prepared from the emulsion with 0.25% free surfactant. Both images suggest an exfoliated structure for the two nanocomposites, which is consistent with the WAXD results. Because of the pressing and shear stress during sample preparation, the clay platelets are well-ordered and almost parallel to the surface of the prepared film.

Figure 8 summarizes the DTG results for the PEA–GP nanocomposites prepared by heterocoagulation method. Incorporation of clay into the rubber matrix does increase the thermal stability, which is common in many polymer–clay nanocomposite systems. We think that the mechanism of thermal stability is the same as we found in poly(methyl methacrylate)–GP nanocomposites,[43] and the DTG patterns are almost the same as those we found in PMMA–GP nanocomposites. Once again, we did not find any significant change of the glass transition temperature of the nanocomposites with respect to the pure rubber.

SUMMARY

Intercalated PEA–clay, PBA–clay, poly(EA-*co*-BA)–clay nanocomposites were prepared by *in situ* polymerization. The thermal stability improvement in PBA–clay nanocomposites is significant and the main decomposition temperature increased by more than 100°C. Exfoliated PEA–clay nanocomposites were ob-

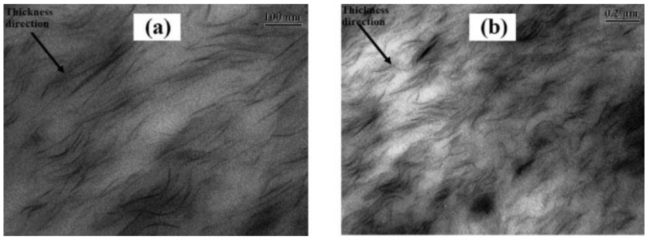

Figure 7 TEM images of PEA–GP nanocomposites from an emulsion with 0.25% free surfactant with respect to monomer: (a) clay loading = 5.85% and (b) clay loading = 9.85%.

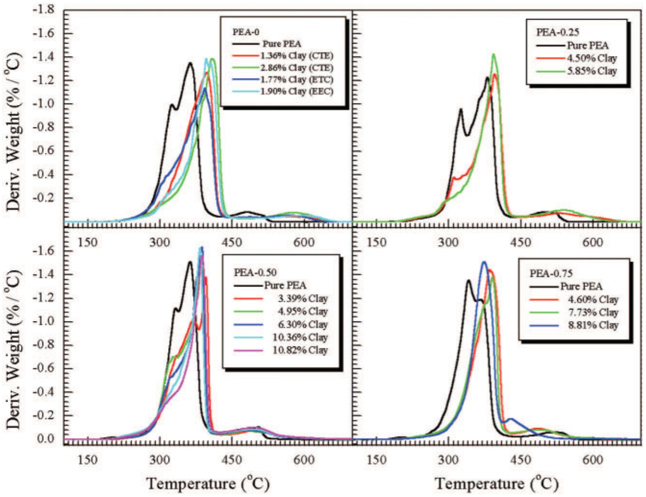

Figure 8 DTG plots for PEA–GP nanocomposites from the emulsions with different amount of free surfactant prepared by heterocoagulation method. [Color figure can be viewed in the online issue, which is available at www.interscience.wiley.com.]

tained by the heterocoagulation method. Both the mixing method and the amount of free surfactant in the emulsion polymerization affect the morphology of the PEA–clay nanocomposites. The emulsion polymerization recipe using 0.25% of free surfactant (with respect to monomer) provided fully exfoliated PEA–GP nanocomposites up to 10% clay loadings. At higher free surfactant loadings, intercalated structures were observed at lower clay loadings and exfoliated structures at higher clay loadings were observed. In all the polyacrylate–clay nanocomposites, no significant changes in the glass transition temperature were observed.

The authors thank Professor Stephen Z. D. Cheng for access to a wide angle X-ray diffractometer.

References

1. Usuki, A.; Kojima, Y.; Kawasumi, M.; Okada, A.; Kurauchi, T.; Kamigaito, O. J Mater Res 1993, 8, 1174.
2. Usuki, A.; Kojima, Y.; Kawasumi, M.; Okada, A.; Kurauchi, T.; Fukushima, Y.; Kamigaito, O. J Mater Res 1993, 8, 1179.
3. Kojima, Y.; Usuki, A.; Kawasumi, M.; Okada, A.; Fukushima, Y.; Kurauchi, T.; Kamigaito, O. J Mater Res 1993, 8, 1185.
4. Giannelis, E. P. Adv Mater 1996, 8, 29.
5. Alexandre, M.; Dubois, P. Mater Sci Eng 2000, 28, 1.
6. Pinnavaia, T. J; Beall, G. W. Polymer-Clay Nanocomposites; Wiley: New York, 2000.
7. Zilg, C.; Dietsche, F.; Hoffman, B.; Dietrich, C.; Mulhaupt, R. Macromol Symp 2001, 169, 65.
8. Vaia, R. A.; Giannelis, E. P. MRS Bull 2001, 26, 394.
9. Schmidt, D.; Shah, D.; Giannelis, E. P. Curr Opin Solid State Mater Sci 2002, 6, 205.
10. Akelah, A.; Salahuddin, N.; Hiltner, A.; Baer, E.; Moet, A. Nanostruct Mater 1994, 4, 965.
11. Lim, S. K.; Lim, S. T.; Kim, H. B.; Chin, I.; Choi, H. J. J Macromol Sci Phys 2003, B42, 1197.
12. Sadhu, S.; Bhowmick, A. K. J Appl Polym Sci 2004, 92, 698.
13. Pramanik, M.; Srivastava, S. K.; Samantaray, B. K.; Bhowmick, A. K. J Appl Polym Sci 2003, 87, 2216.
14. Sadhu, S.; Bhowmick, A. K. J Polym Sci Part B: Polym Phys 2004, 42, 1573.
15. Kojima, Y.; Fukumori, K.; Usuki, A.; Okada, A.; Kurauchi, T. J Mater Sci Lett 1993, 12, 889.
16. Lopez-Manchado, M. A.; Arroyo, M.; Herrero, B.; Biagiotti, J. J Appl Polym Sci 2003, 89, 1.
17. Arroyo, M.; Lopez-Manchado, M. A.; Herrero, B. Polymer 2003, 44, 2447.
18. Varghese, S.; Karger-Kocsis, J.; Gatos, K. G. Polymer 2003, 44, 3977.
19. Wu, Y. P.; Ma, Y.; Wang, Y. Q.; Zhang, L. Q. Macromol Mater Eng 2004, 289, 890.
20. Teh, P. L.; Mohd Ishak, Z. A.; Hashim, A. S.; Karger-Kocsis, J.; Ishiaku, U. S. Eur Polym J 2004, 40, 2513.
21. Nah, C.; Ryu, H. J.; Han, S. H.; Rhee, J. M.; Lee, M. H. Polym Int 2001, 50, 1265.
22. Kim, J. T.; Lee, D. Y.; Oh, T. S.; Lee, D. H. J Appl Polym Sci 2003, 89, 2633.
23. Ganter, M.; Gronski, W.; Semke, H.; Zilg, T.; Thomann, C.; Muhlhaupt, R. Kautsch Gummi Kunstst 2001, 54, 166.
24. Ganter, M.; Gronski, W.; Reichert, P.; Mulhaupt, R. Rubber Chem Technol 2001, 74, 221.
25. Mousa, A.; Karger-Kocsis, J. Macromol Mater Eng 2001, 286, 260.
26. Privalko, V. P.; Ponomarenko, S. M.; Privalko, E. G.; Schon, F.; Gronski, W.; Staneva, R.; Stuhn, B. Macromol Chem Phys 2003, 204, 1480.
27. Hasegawa, N.; Okamoto, H.; Usuki, A. J Appl Polym Sci 2004, 93, 758.
28. Liang, R.; Wang, Y.; Wu, Y.; Lu, Y.; Zhang, H.; Zhang, L. Polym Test 2005, 24, 12.
29. Feng, W.; Ait-Kadi, A.; Riedl, B. Macromol Rapid Commun 2002, 23, 703.
30. Wang, S.; Long, C.; Wang, X.; Li, Q.; Qi, Z. J Appl Polym Sci 1998, 69, 1557.
31. Lebaron, P. C.; Pinnavaia, T. J. Chem Mater 2001, 13, 3760.
32. Ma, J.; Zhang, S.; Qi, Z. J Appl Polym Sci 2001, 82, 1448.
33. Chen, Z.; Huang, C.; Liu, S.; Zhang, Y.; Gong, K. J Appl Polym Sci 2000, 75, 796.
34. Ray, S.; Bhowmick, A. K. Rubber Chem Tech 2001, 74, 835.
35. Tong, X.; Zhao, H.; Tang, T.; Feng, Z.; Huang, B. J Polym Sci Part A: Polym Chem 2002, 40, 1706.
36. Wang, Z.; Zhang, L.; Tang, C.; Yu, D. J Appl Polym Sci 2000, 78, 1879.
37. Wu, Y.; Zhang, L.; Wang, Y.; Liang, Y.; Yu, D. J Appl Polym Sci 2001, 82, 2842.
38. Wu, Y.; Jia, Q.; Yu, D.; Zhang, L. J Appl Polym Sci 2003, 89, 3855.
39. Varghese, S.; Karger-Kocsis, J. Polymer 2003, 44, 4921.
40. Varghese, S.; Gatos, K. G.; Apostolov, A. A.; Jarger-Kocsis, J. J Appl Polym Sci 2004, 92, 543.
41. Ma, J; Xiang, P.; Mai, Y.; Zhang, L. Macromol Rapid Commun 2004, 25, 1692.
42. Huang, X.; Brittain, W. J. Macromolecules 2001, 34, 3255.
43. Xu, Y.; Brittain, W. J.; Xue, C.; Eby, R. K. Polymer 2004, 45, 3735.
44. Lee, S. H.; Brittain, W. J., Unpublished results.